# ANALYTICAL INVESTIGATION OF A PRE-COOLED HEAT PUMP FOR HVAC APPLICATIONS USING THE MAISOTSENKO CYCLE

Javier Ruiz Ramírez[1,*], Clara Gascó Arranz[1], Michael Opolot[2], Sangkyoung Lee[3], Chunrong Zhao[4]

[1]Engineering Research Institute of Elche, Miguel Hernández University, Elche, Spain
[2]Centre for Hydrogen & Renewable Energy, Central Queensland University, Gladstone, Australia
[3]School of Mechanical and Mining Engineering, The University of Queensland, Brisbane, Australia
[4]School of Aerospace, Mechanical and Mechatronic Engineering, The University of Sydney, Australia

*Corresponding Author: j.ruiz@umh.es

## ABSTRACT

Highly-efficient heat pump systems can significantly reduce the energy use in buildings, thereby contributing to meet Europe's climate commitments, including building decarbonisation by 2050. The Maisotsenko Cycle (M-cycle onwards) is an indirect, multi-stage type of evaporative cooling which can be used in different air-conditioning applications. The use of the M-cycle to pre-cool the inlet air of the condenser in a heat pump constitutes an strategy that has not been explored in the reviewed literature. In this sense, this study addresses the hybridisation of a heat pump for air conditioning applications along with an Maisotsenko cooler (M-cooler). The main novelty of the system relies on the use of the M-cooler to pre-cool the air entering the condenser of the heat pump rather employing it to meet, totally or partially, the thermal load of the building. This study constitutes a preliminary approach for assessing the suitability of using an M-cooler to enhance the performance of an air-air heat pump via pre-cooling the inlet air to its condenser.

An analytical model of a building and cooling system consisting of a heat pump and a M-cooler was developed to investigate the impact of enhancing heat pump performance through pre-cooling the air entering its condenser. The models for the system components and the building model were validated with experimental data, showing a good agreement. An comparative analysis based on the total power consumption (fan and compressor) as key performance indicator was conducted. During the hottest day of the year in Alicante, where the building is located, the system peak consumption decreases from 1.8 to 1.2 kW when the pre-cooling is activated. This translates into a 33.7% reduction. The calculated improvement ratio for a typical summer day is 1.5% $^{\circ}C^{-1}$, which is in agreement with the results reported by other authors that have used evaporative pre-cooling techniques in the condenser of a heat pump. The simulation conducted for the summer period (June, July, August and September) showed a potential benefit of 17% in the energy use for air-conditioning purposes. The average EER of the heat pump is increased from 3.92 to 4.65 (18.64%).

This study provides valuable insights for the design and implementation of efficient cooling technologies, advancing beyond previous efforts in the literature.

## 1 INTRODUCTION

According to the International Energy Agency (IEA), emissions from the buildings sector have been steadily increasing, averaging a 1% rise per year since 2015. Alarmingly, this sector alone accounts for over one-third of the total global emissions. A substantial portion of these emissions stems from the


https://doi.org/10.52202/077185-0119

energy-intensive task of maintaining comfortable indoor conditions. As temperatures continue to rise due to the effects of climate change, coupled with rapid economic development and urbanisation in the world's hottest regions, the demand for cooling solutions is expected to surge. Conventional mechanical vapour-compression air-conditioning systems consume significant amount of electrical energy that is largely, primarily reliant on fossil fuels, thereby contributing to the increase of $CO_2$ emissions. In this context, exploring innovative approaches to mitigate the environmental impact of the space cooling becomes crucial.

The use of evaporative pre-cooling methods on the condenser of a refrigeration, heat pump-based system presents a remarkably efficient and easily implementable approach to increase the performance of air conditioning systems worldwide, especially in regions characterised by hot and dry climates (Martínez et al., 2016). These methodologies enable a substantial decrease in the energy use and the mitigation of peak energy demands by introducing a minimal amount of water for a limited period to cool the incoming air.

The Maisotsenko cycle (M-cycle onwards), or indirect dew-point evaporative cooler, distinguishes itself by its capability to cool air to the dew-point temperature rather than the wet-bulb temperature achieved by direct evaporative cooling methods. Additionally, the M-cycle boasts a lower energy requirement for operation. This cycle is characterised as an indirect, multi-stage type of evaporative cooling system, leveraging the psychrometric renewable energy available from the latent heat of water evaporating into the air. In the M-cycle, ambient air is drawn into a dry channel, where it releases sensible heat to a wet channel. As a result, the outlet air leaving the system is cooler than the ambient temperature. It proves advantageous to redirect a portion of this air to serve as the working air in the wet channel. This working air is then humidified and absorbs heat from the dry channel before being expelled into the atmosphere. Consequently, the outlet air temperature is lowered below the ambient wet bulb temperature without altering humidity levels.

Numerous studies have investigated the potential of indirect dew-point evaporative coolers for space cooling. For instance, Pandelidis, Anisimov, and Worek (2015) developed a two-dimensional M-Cycle cross-flow heat exchanger model, shedding light on their performance under various operational conditions. Their findings underscore the influence of factors such as inlet air parameters, design features, and system configurations on energy efficiency and effectiveness, thereby highlighting the significant potential of these devices in air-conditioning systems. Similarly, Boukhanouf et al. (2017) presented a computer and experimental model of a sub-wet bulb temperature indirect evaporative cooling system for space cooling in buildings, achieving a cooling capacity of 225 W/m$^2$. Caliskan et al. (2011) made an energetic, exegetic and sustainability analysis of the M-cycle compared with three conventional types of air cooling systems for building applications, obtaining better results for the M-cycle. Researching about the design of the evaporative cooler, Oh et al. (2019) developed a mathematical model of the indirect evaporative cooler to compare the performances between a single-purge and four-purge configuration. Kabeel et al. (2017) modified the heat exchanger adding internal baffle, finding significant improvements in supply air temperature reduction (21%) and coefficient of performance (71%) compared to previous designs. Zhao et al. (2009) investigated the feasibility of dew point evaporative cooling for air conditioning in Chinese and UK regions. They conclude that the system is suitable for most areas, particularly those with hot, dry climates, while adaptation measures are needed for humid regions. They also find tap water temperature adequate to feed the system. Similarly, Jaber and Ajib (2011) studied its feasibility in Mediterranean regions with two different configurations, concluding of its high potential and high energy and economic savings. On the same line, Pandelidis, Anisimov, Drąg, et al. (2018) used Polish climate data to compare the performance of the typical air conditioning systems and without the M-cycle, concluding that evaporative cooling through Maisotsenko cycle has high application potential and allows to generate significant energy savings.

Another line of investigation has been the hybridisation of cooling systems, integrating indirect evaporative coolers, as it presents an avenue for significant energy savings and performance improvements. For instance, Liu et al. (2018) presented two hybrid cooling systems combining dew-point evaporative



https://doi.org/10.52202/077185-0119

coolers with heat pipes for computing and data centre cooling systems, leading to nearly 90% of annual energy savings compared with vapour compression refrigeration. Similarly, Zanchini and Naldi (2019) coupled the M-cycle to a conventional refrigeration cycle, comparing its performance with a traditional system. The results showed that the application of the M-cycle to the heat recovery yielded a 38% reduction in the total use of electric energy.

The use of an M-cycle to pre-cool the inlet air of the condenser in a heat pump constitutes an strategy that has not been explored in the reviewed literature. This is the research gap filled by this investigation. This study addresses the hybridisation of a heat pump for air conditioning applications along with an M-cooler. The main novelty of the system relies on the use of the M-cooler to pre-cool the air entering the condenser of the heat pump rather employing it to meet, totally or partially, the thermal load of the building. It consists of a preliminary approach for assessing the suitability of using an M-cooler to enhance the performance of an air-air heat pump via pre-cooling the inlet air to its condenser.

This paper is organised as follows: Section 2 details the models used in the analysis and how the are connected. Next, the validation of the models and the results of the performance of the system are presented and discussed in Section 3. Finally, the the most important findings of the research are summarised in Section 4.

## 2 METHODOLOGY

This section includes the generated models for the M-cooler, the air-conditioning heat pump, and the building, and the interaction between them.

### 2.1 M-cycle modelling

A detailed mathematical model of the M-cycle has been developed. To simplify the analysis, the following assumptions were made:

- There are no heat losses to the surroundings.
- The thermal resistance of the wall and temperature difference of wall surfaces between the dry and wet side are neglected because of the thickness of the plate.
- Air is considered an incompressible fluid; hence, all its properties are uniform within the incremental control volume.
- The secondary air stream is assumed to be equally saturated with the water film.
- The Lewis number is equal to 1 (Le=1), as suggested by other authors, (Sadighi Dizaji et al., 2018).

Figure 1 shows a schematic description of the M-cycle model. The equations that describe the thermophysical processes occurring in the indirect evaporative cooler are defined for a differential control volume through the following equations.

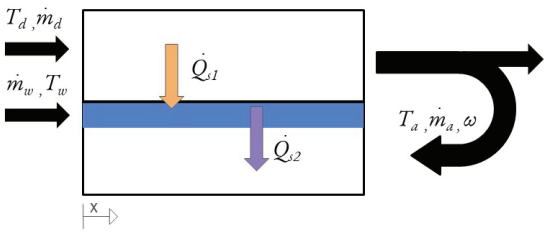


**Figure 1:** Schematic description of the M-cycle model.


https://doi.org/10.52202/077185-0119

On the one hand, along the dry channel there is only sensible heat transfer taking place from the air primary stream to the water film on the wet channel:

$$d\dot{Q}_{s_1} = h_{c_d} a (T_d - T_w) dx \tag{1}$$

On the other hand, along the wet channel both sensible and latent heat transfers occur between the water film and the air stream, along with mass transfer due to water evaporating into the air stream:

$$d\dot{Q}_{s_2} = h_c a (T_w - T_a) dx \tag{2}$$

$$d\dot{Q}_L = h_{Lv} d\dot{m}_w = -h_{Lv} d\dot{m}_v \tag{3}$$

$$d\dot{m}_w = -h_m \rho_w a (\omega_s - \omega) dx \tag{4}$$

Where the mass transfer coefficient between the secondary air stream and the water film is represented by a function of the Lewis number and the convective heat transfer coefficient, as follows:

$$h_m \rho_v = \frac{h_c}{c_{p_h} \mathrm{Le}} \tag{5}$$

Overall, by applying energy and mass balances to the different control volumes (dry channel, water film, and secondary air stream), we derive a differential nonlinear system comprising five equations. First equation is the energy balance on the dry channel, where the difference on the enthalpy of the air stream is due to the loss of sensible heat.

$$\dot{m}_d c_{p_h} dT_d = -d\dot{Q}_{s_1} \tag{6}$$

Second equation is the energy balance on the water film. The water enthalpy difference for a differential volume is caused by the exchange of sensible heat between the air stream on the primary channel (gain of heat) and the exchange of sensible and latent heat with the air stream of the secondary channel.

$$\dot{m}_w c_{p_w} dT_w = -d\dot{Q}_{s_2} + d\dot{Q}_{s_1} - d\dot{Q}_L \tag{7}$$

Third equation is the energy balance on a differential volume of the air stream of the secondary channel. The air stream enthalpy difference is a result of the sensible heat transfer with the water film.

$$\dot{m}_a c_{p_h} \frac{dT_d}{dx} = d\dot{Q}_{s_2} \tag{8}$$

The fourth equation is the mass balance on a differential volume of the air stream on the secondary channel. The equation describes how the humidity ratio changes along the wet channel as a result of water evaporation relative to the mass flow rate of dry air.

$$d\omega = \frac{d\dot{m}_v}{\dot{m}_a} = \frac{h_m \rho_v a}{\dot{m}_a} (\omega_s - \omega) dx \tag{9}$$

The fifth equation is the mass balance applied to a differential volume of the water film. The loose of water is equal to the gain of water vapour on the air stream ($d\dot{m}_w = \dot{m}_a d\omega$). Substituting terms and rearranging equations, the system reached is shown in Equation (10) . This system is solved by means of numerical methods. Consequently, the developed model provides predictions for the temperature evolution of the primary and secondary air streams and the water, along with the humidity variation of the secondary air stream and the water mass flow along the secondary channel.



https://doi.org/10.52202/077185-0119

$$
\begin{aligned}
\frac{dT_d}{dx} &= \frac{h_{c_d} a}{\dot{m}_d c_{p_h}} (T_d - T_w) \\
\frac{dT_w}{dx} &= -\frac{h_c a}{\dot{m}_w c_{p_w}} (T_w - T_a) + \frac{h_{c_d} a}{\dot{m}_w c_{p_w}} (T_d - T_w) - \frac{h_c a h_{L_v}}{\dot{m}_w c_{p_w} c_{p_h} \mathrm{Le}} (\omega_s - \omega) \\
\frac{dT_a}{dx} &= -\frac{h_c a}{\dot{m}_a c_{p_h}} (T_w - T_a) \\
\frac{d\omega}{dx} &= -\frac{h_c a}{\dot{m}_a c_{p_h} \mathrm{Le}} (\omega_s - \omega) \\
d\dot{m}_w &= \dot{m}_a d\omega
\end{aligned} \tag{10}
$$

Additionally, to drive the system there is a need to use a fan to overcome the total pressure drop of the heat exchanger. The pressure drop of the airflow is due to the frictional losses, which can be estimated with the Darcy-Weisbach equation. The total power consumption of the fan is calculated as follows:

$$\dot{W}_f = \frac{\Delta p Q}{\eta_f} \tag{11}$$

The wet-bulb effectiveness is the ratio of the difference between intake and outlet air temperature to the difference between intake air temperature and its wet bulb temperature. This can be expressed as:

$$\varepsilon_{wb} = \frac{T_{\text{in}} - T_{\text{out}}}{T_{\text{in}} - T_{wb}} \tag{12}$$

Similarly, the dew-point effectiveness is defined as the ratio of the difference between intake and outlet air temperature to the difference between intake air temperature and its dew point temperature:

$$\varepsilon_{dp} = \frac{T_{\text{in}} - T_{\text{out}}}{T_{\text{in}} - T_{dp}} \tag{13}$$

The description of the geometric and operation characteristics of the M-cooler considered in this paper can be found in Riangvilaikul and Kumar (2010).

### 2.2 Heat pump modelling

The performance of a heat pump is usually described by the Energy Efficiency Ratio (EER), Eq. (14), which measures the ratio of cooling power to electrical power.

$$\text{EER} = \frac{\dot{Q}_{\text{evap}}}{\dot{W}_{\text{comp}}} \tag{14}$$

As noted by F. Aguilar et al. (2017) and Underwood et al. (2017) among others, the EER is primarily influenced by the condensation and evaporation temperatures ($T_{\text{cond}}$ and $T_{\text{evap}}$), as well as the Load Factor (LF), which is the ratio of the actual to maximum capacity. From the experimental data presented by F. Aguilar et al. (2017), it was determined that the EER is dependent on the condenser-evaporator temperature difference ($\Delta T_{\text{cond-evap}}$) and the load factor. For convenience in this study, the indoor-outdoor temperature difference ($\Delta T_{\text{in-out}}$) was used instead of $\Delta T_{\text{cond-evap}}$. This is justified since pair of temperatures $T_{\text{out}} - T_{\text{cond}}$ and $T_{\text{in}} - T_{\text{evap}}$ are linked via the heat exchange thermal approach. In accordance with EnergyPlus (2021), the EER was correlated using a standard two-variable equation, shown in Equation (15):

$$\text{EER} = a_1 + a_2 \Delta T_{\text{in-out}} + a_3 \text{LF} + a_4 \Delta T_{\text{in-out}} \text{LF} + a_5 \text{LF}^2 \tag{15}$$

Constants $a_{1-5}$ were derived by fitting Equation (15) to the experimental data from F. Aguilar et al. (2017), and are listed in in Table 1. The fitting coefficients were determined with 95% confidence intervals.


https://doi.org/10.52202/077185-0119

**Table 1:** Constants $a_n$ in Equation (15).

| $n$ | 1 | 2 | 3 | 4 | 5 |
|---|---|---|---|---|---|
| | 5.7055 | -0.0474 | 4.3236 | -0.0009 | -7.1835 |

### 2.3 Building modelling

A detailed description of the building model can be found in F. J. Aguilar et al. (2021). The geometric modeling of the building was performed using the LIDER/CALENER unified computer tool (HULC).

This model encompasses a 3D representation of the building within the energy analysis software. It also includes the definition of the building's primary architectural parameters, such as the dimensions (floor plans and height), the layout of interior spaces, and the composition of the opaque and transparent thermal envelopes. The opaque envelope comprises walls, roofs, floors, and insulation, while the transparent envelope includes windows, skylights, and glass doors. HULC is the official tool used in Spain for both ensuring compliance with building regulations and for the energy certification of buildings. It features the DOE-2 calculation engine, one of the most renowned energy analysis software packages globally. Using experimental data, building plans, and on-site measurements, the building's characteristic parameters were defined, considering factors like thermal insulation, usage patterns, and internal thermal loads (occupancy, lighting, and equipment). It was determined that the thermal envelope includes a double-layer facade with a 4-millimetre thermal insulation layer. The glazed areas feature $3 \times 1.5$ m$^2$ double-glazed windows (4/6/4) equipped with sunshade slats. The ceiling height is 2.8 m, and the installed lighting power is 14 W/m$^2$ with fluorescent technology. The building is used continuously for 12 hours daily, from 8 AM to 8 PM. The main facade faces west, and there is another office building adjacent to the east side. To the south, an industrial building provides shade at certain times of the year, while the north facade is fully exposed. Photovoltaic panels on the roof also create shade on the building. All of this information was incorporated into the 3D model of the building.

### 2.4 Interaction between models

The global model requires 3 ambient variables as inputs: ambient temperature ($T_\infty$), ambient relative humidity ($\phi_\infty$) and global irradiance ($G$). The global model predicts the operating parameters of each subsystem (i.e. cooling demand, outlet air temperature in the M cooler, heat pump EER) and the global key performance indicators (compressor and fan power consumption). The interaction between models is depicted in Figure 2.

In the first step, the equations for the M-cycle model are solved iteratively. The main output provided by the model is outlet air temperature ($T_{\text{out}}$). Afterwards, the cooling loads are predicted using the building model. Finally, the heat pump model is fed by the cooling load and the air temperature provided by the M-cooler to calculate the EER. As a result, the power used by the fan in the M-cooler and the compressor of the heat pump are determined.

## 3 RESULTS AND DISCUSSION

### 3.1 Experimental validation

The models presented in Section 2 was validated using two different sets of experimental results. The experimental results presented in F. Aguilar et al. (2017) were used to validate the building and heat pump models. In this study, the authors experimentally analysed the performance of a PV-driven, air-air heat pump used to meet the cooling demand of an office located in Elche (Alicante). The heat pump used in their setup had a nominal cooling capacity of 3.52 kW. Seventeen different magnitudes were measured every 5 minutes during 6 months. Consequently, the necessary variables for validating the building and heat pump models were available.



https://doi.org/10.52202/077185-0119

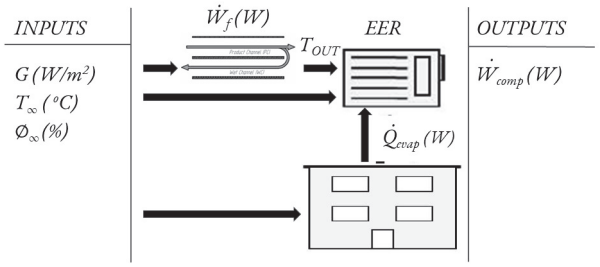


**Figure 2:** Schematic representation of the interaction building-system.

On the other hand, the experimental results reported by Riangvilaikul and Kumar (2010) were employed to assess the goodness of the M-cooler model. In this paper, the performance of an M-cooler was experimentally characterised. The authors reported performance values for the cooler operating under different inlet air conditions (temperature, humidity and velocity)

3.1.1 M-cooler model validation: Figure 3 displays the validation of the M-cycle model. It contains the experimental data reported by Riangvilaikul and Kumar (2010). The authors conducted 18 experiments, where the inlet air temperature ($T_{\text{in}}$) was varied in 5 levels (ranging from 25 to 45 in 5ºC intervals) and the inlet air absolute humidity ($\omega_{\text{in}}$) was modified in 4 levels (0.0069, 0.0112, 0.02 and 0.0264 $\text{kg}_v/\text{kg}_a$). The results provided by the model show differences of less than 1.5% compared to those published in the literature in terms of the outlet air temperature for the 18 cases compared.

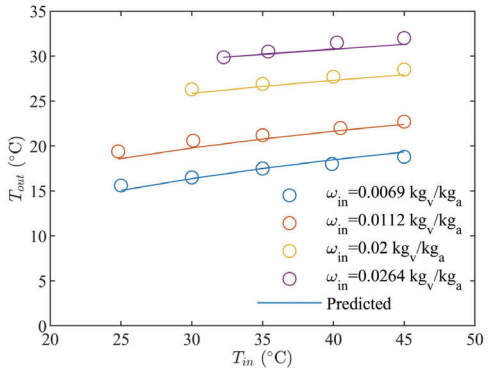


**Figure 3:** Comparison between experimental (Riangvilaikul and Kumar, 2010) and predicted results. M-cycle model.

3.1.2 Building model validation: Figure 4 presents a comparison of the cooling thermal demand for the summer months (June, July, August, and September) between the predictions made by the building model and the experimental measurements. As shown, the predicted results for July and August align very closely with the experimental data, with differences of less than 5%. The reported results for June and September, however, are underpredicted when compared to the observed values. However, the results for June and September are underestimated when compared to the observed values. This discrepancy may be attributed to the actual experimental climatic conditions during these months being more severe than those assumed in the simulation tool.


https://doi.org/10.52202/077185-0119

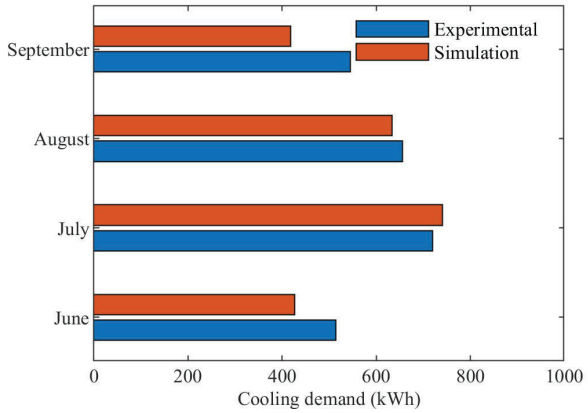


**Figure 4:** Comparison between monthly experimental and predicted results. Building model.

3.1.3 Heat pump model validation: Figures 5 shows the experimental validation of the developed model for the heat pump.

Figure 5(a) presents the comparison between the experimental (solid) and predicted (dashed) power consumption values for two different summer days: the $31^{st}$ of July and the $2^{nd}$ of August. Those days were chosen because they offered completely different information concerning heat demand profiles, so the accuracy of the developed model could be tested. The $31^{st}$ of July had the main thermal demand during the morning hours, and the energy consumption decreased at noon. During the $2^{nd}$ of August, the thermal demand was higher and was mainly concentrated in the afternoon. As it can be seen, the results predicted by the heat pump model are in good agreement with the experimental results. The total energy consumed by the air conditioning unit was 5.7 kWh for the $31^{st}$ of July and 8.4 kWh for the $2^{nd}$ of August. Taking into account the total daily cooling demand and the power consumption, the EER of the heat pump on the $31^{st}$ of July was 9.9, while on the $2^{nd}$ of August was 7.0.

Figure 5(b) illustrates the relative error when predicting the instant overall power consumption on the $31^{st}$ of July using the developed model compared to the experimental results. The average relative error is 4.15% while the maximum relative error is equal to 13.40%.

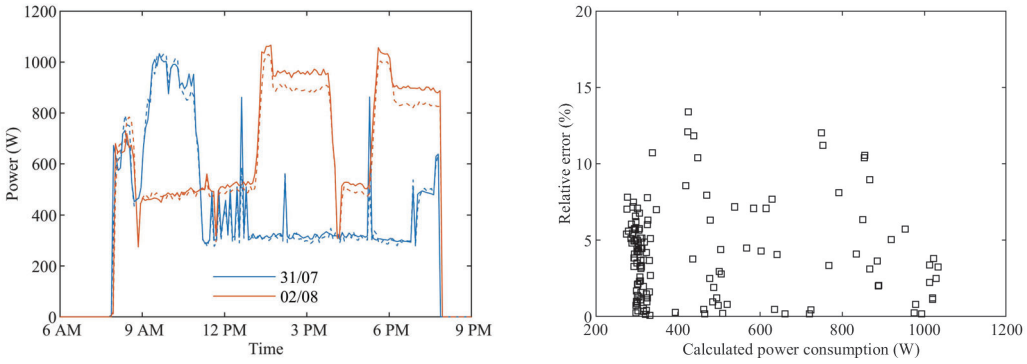


(a) Daily variation of $\dot{W}_{\text{comp}}$.

(b) Relative error overall power consumption

**Figure 5:** Heat pump model validation.(a) Experimental (solid), and simulated (dashed) electrical curves registered along the $31^{st}$ of July and the $2^{nd}$ of August. (b) Relative error between predicted and experimental overall power consumption.



https://doi.org/10.52202/077185-0119

### 3.2 Effect of pre-cooling the inlet air to the condenser

This section presents the results of the operation of the pre-cooled heat pump system in the building during the summer months.

Figure 6 shows the daily evolution of the ambient conditions and the system (heat pump and M-cycle) operating conditions during the hottest day of the year in Alicante ($21^{st}$ July).

Figure 6(a) presents the evolution of ambient conditions. The difference between the ambient temperature and the M-cycle outlet temperature varies with the ambient humidity. The lower the humidity, the higher the cooling potential. At 3 pm, when the ambient temperature is 41.1ºC and the relative humidity is 18.2%, the M-cooler outlet temperature is approximately 19ºC, which implies that the system reduces the temperature 22ºC. This figure also includes the variation of the wet-bulb and dew-point temperatures. As it can be seen, the outlet temperature is below the ambient air wet-bulb temperature. The calculated daily averaged wet-bulb and dew-point effectivenesses are 1.167 and 0.762.

Figure 6(b) shows the variation of the power required to drive the compressor of the heat pump and the fan of the M-cooler and its EER. Two sets of series are included in the figure: original configuration of the HVAC system (heat pump with no pre-cooling) and when the inlet air to the condenser is pre-cooled with the M-cooler. This figure is plotted from 6 AM to 3 PM because this is the period when the building has cooling demand. The power required to drive the compressor is reduced when the pre-cooling is utilised. The peak value decreases from 1.8 to 1.2 kW, which translates into a 33.7% reduction. The temperature drop in the M-cooler to achieve this benefit is ~20ºC, which leads to an improvement ratio of 1.5% $ºC^{-1}$. This value is in agreement with the results reported by other authors that have used evaporative pre-cooling techniques in the condenser of a heat pump (Martínez et al., 2016). The energy consumption decreases from 7.62 to 5.82 kWh. As the cooling demand is 22.92 kWh, the daily EER is increased from 3 to 3.93 (31%). The energy required to drive the fan was approximately 30 W (assuming a 75% fan efficiency), which is negligible compared to the compressor consumption.

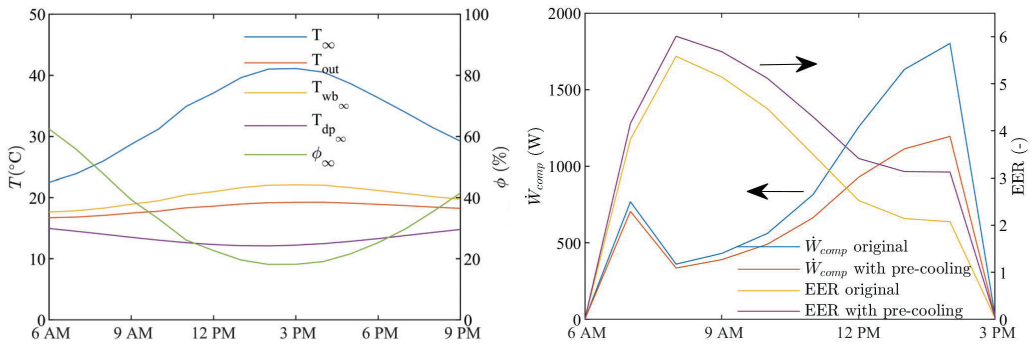


(a) Daily variation of ambient conditions.

(b) Daily variation of $\dot{W}_{\text{comp}}$.

**Figure 6:** (a) Variation of ambient conditions during the $21^{st}$ of July. (b) Variation of heat pump and M-cooler performance during the $21^{st}$ of July.

Figure 7 shows the results of the previous comparative analysis extended to the summer months. The effect of pre-cooling the air involves a energy reduction of 100 kWh, from 592.27 to 491.92 kWh (16.95%). This difference is more evident in July and August when the cooling requirements are higher. This figure also includes the variation of the monthly EER for the system proposed in this investigation and the system without pre-cooling. On average, the EER is improved by 18.64%, from 3.92 to 4.65.


https://doi.org/10.52202/077185-0119

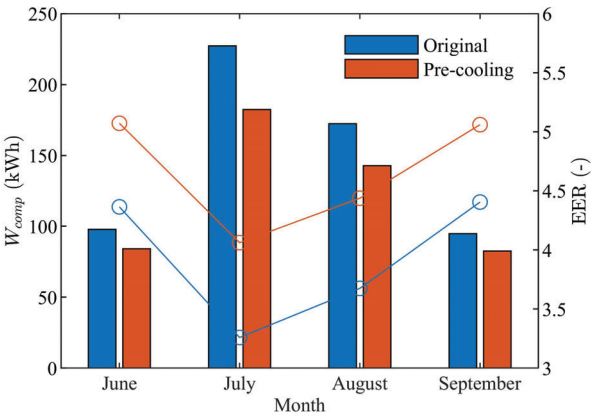


**Figure 7:** Comparison between the predicted results by the model in terms of energy consumption for the summer months.

## 4 CONCLUSIONS

An analytical investigation was conducted in this study to assess the impact of pre-cooling the inlet air to the condenser of a heat pump used to meet the cooling requirements of an office building. The main novelty is the use of an indirect dew-point evaporative cooler (Maisotsenko cycle) to pre-cool the air. The results obtained during the investigation can be summarised as follows.

- The analytical models of the different components of the system (air-air heat pump and M-cycle) and the building model have been linked and the predicted results have been validated with experimental data, showing a good agreement.
- The use of the M-cycle to pre-cool the inlet condenser air enhances the performance of the system. The average improvement is roughly 1.5% $^{o}C^{-1}$, which is in agreement with the values reported in the literature obtained for other pre-cooling approaches. As the M-cycle achieves greater temperature reductions than conventional evaporative systems, the power requirements are much lower. The reduction in the annual energy consumption can be up to 17%.
- This is a preliminary investigation to assess the potential of this approach. The results obtained consider that the pre-cooling system operates non-stop and at full capacity. It has been found that there are several hours during the summer months where the benefit of pre-cooling is small, mainly due to high ambient relative humidities. Therefore, an optimisation analysis concerning the M-cooler operation could increase the reported improvements.
- As a final remark, the water consumption should be obtained to compare the relative performance of the system including this water use with other evaporative pre-cooling systems.


https://doi.org/10.52202/077185-0119

## NOMENCLATURE

| | |
|---|---|
| $a$ | channel width, m |
| $c_p$ | specific heat, J kg$^{-1}$ K$^{-1}$ |
| $\Delta p$ | pressure drop, Pa |
| $\Delta T$ | temperature difference, ºC |
| $G$ | global irradiance, W m$^{-2}$ |
| $h_c$ | convective heat transfer coefficient, W m$^{-2}$ K$^{-1}$ |
| $h_m$ | mass transfer coefficient, m s$^{-1}$ |
| $L$ | channel length, m |
| Le | Lewis number |
| $\dot{m}$ | mass flow rate, kg s$^{-1}$ |
| $Q$ | volumetric flow rate, m$^3$ s$^{-1}$ |
| $\dot{Q}$ | heat rate, W |
| $\dot{Q}_L$ | latent heat transfer rate, W |
| $\dot{Q}_S$ | sensible heat transfer rate, W |
| $r$ | working air to intake mass flow ratio |
| $T$ | Temperature, ºC |
| $\dot{W}$ | power consumption, W |
| $x$ | distance of the differential element, m |

### Abbreviations

| | |
|---|---|
| EER | Energy Efficiency Ratio |

### Latin Symbols

| | |
|---|---|
| $\varepsilon$ | effectiveness |
| $\eta$ | efficiency |
| $\rho$ | density, kg m$^{-3}$ |
| $\phi$ | relative humidity |
| $\omega$ | humidity ratio |
| $\omega_s$ | saturation humidity ratio |

### Superscripts and Subscripts

| | |
|---|---|
| $a$ | secondary channel air stream |
| cond | condenser |
| comp | compressor |
| $d$ | primary channel air stream |
| dp | dew point |
| evap | evaporator |
| $f$ | fan |
| $h$ | humid air |
| in | inlet |
| out | outlet |
| $v$ | water vapour |
| $w$ | water |
| wb | wet bulb |

## REFERENCES

Aguilar, F., S. Aledo, and P. Quiles (2017). "Experimental analysis of an air conditioner powered by photovoltaic energy and supported by the grid". In: *Applied Thermal Engineering* 123, pp. 486–497. ISSN: 1359-4311. DOI: https://doi.org/10.1016/j.applthermaleng.2017.05.123. URL: https://www.sciencedirect.com/science/article/pii/S1359431116338194.

Aguilar, F. J. et al. (2021). "Performance Analysis and Optimisation of a Solar On-Grid Air Conditioner". In: *Energies* 14.23. DOI: 10.3390/en14238054. URL: https://www.mdpi.com/1996-1073/14/23/8054.



https://doi.org/10.52202/077185-0119

Boukhanouf, R. et al. (2017). "Computer modelling and experimental investigation of building integrated sub-wet bulb temperature evaporative cooling system". In: *Applied Thermal Engineering* 115, pp. 201–211. ISSN: 1359-4311. DOI: https://doi.org/10.1016/j.applthermaleng.2016.12.119. URL: https://www.sciencedirect.com/science/article/pii/S1359431116343964.

Caliskan, H., I. Dincer, and A. Hepbasli (2011). "Exergetic and sustainability performance comparison of novel and conventional air cooling systems for building applications". In: *Energy and Buildings* 43.6, pp. 1461–1472. ISSN: 0378-7788. DOI: https://doi.org/10.1016/j.enbuild.2011.02.006. URL: https://www.sciencedirect.com/science/article/pii/S0378778811000508.

Jaber, S. and S. Ajib (2011). "Evaporative cooling as an efficient system in Mediterranean region". In: *Applied Thermal Engineering* 31.14, pp. 2590–2596. ISSN: 1359-4311. DOI: https://doi.org/10.1016/j.applthermaleng.2011.04.026. URL: https://www.sciencedirect.com/science/article/pii/S1359431111002249.

Kabeel, A. et al. (2017). "Performance improvement of a hybrid air conditioning system using the indirect evaporative cooler with internal baffles as a pre-cooling unit". In: *Alexandria Engineering Journal* 56.4, pp. 395–403. ISSN: 1110-0168. DOI: https://doi.org/10.1016/j.aej.2017.04.005. URL: https://www.sciencedirect.com/science/article/pii/S1110016817301473.

Liu, Y. et al. (2018). "Energy savings of hybrid dew-point evaporative cooler and micro-channel separated heat pipe cooling systems for computer data centers". In: *Energy* 163, pp. 629–640. ISSN: 0360-5442. DOI: https://doi.org/10.1016/j.energy.2018.07.172. URL: https://www.sciencedirect.com/science/article/pii/S0360544218314695.

Martínez, P. et al. (2016). "Experimental study on energy performance of a split air-conditioner by using variable thickness evaporative cooling pads coupled to the condenser". In: *Applied Thermal Engineering* 105, pp. 1041–1050. ISSN: 1359-4311. DOI: https://doi.org/10.1016/j.applthermaleng.2016.01.067. URL: https://www.sciencedirect.com/science/article/pii/S1359431116300175.

Oh, S. J. et al. (2019). "Approaches to energy efficiency in air conditioning: A comparative study on purge configurations for indirect evaporative cooling". In: *Energy* 168, pp. 505–515. ISSN: 0360-5442. DOI: https://doi.org/10.1016/j.energy.2018.11.077. URL: https://www.sciencedirect.com/science/article/pii/S0360544218322886.

Pandelidis, D., S. Anisimov, P. Drąg, et al. (2018). "Analysis of application of the M-Cycle heat and mass exchanger to the typical air conditioning systems in Poland". In: *Energy and Buildings* 158, pp. 873–883. ISSN: 0378-7788. DOI: https://doi.org/10.1016/j.enbuild.2017.10.052. URL: https://www.sciencedirect.com/science/article/pii/S0378778817312434.

Pandelidis, D., S. Anisimov, and W. M. Worek (2015). "Performance study of the Maisotsenko Cycle heat exchangers in different air-conditioning applications". In: *International Journal of Heat and Mass Transfer* 81, pp. 207–221. ISSN: 0017-9310. DOI: https://doi.org/10.1016/j.ijheatmasstransfer.2014.10.033. URL: https://www.sciencedirect.com/science/article/pii/S0017931014009181.

Riangvilaikul, B. and S. Kumar (2010). "An experimental study of a novel dew point evaporative cooling system". In: *Energy and Buildings* 42.5, pp. 637–644. ISSN: 0378-7788. DOI: https://doi.org/10.1016/j.enbuild.2009.10.034. URL: https://www.sciencedirect.com/science/article/pii/S0378778809002837.

Sadighi Dizaji, H. et al. (2018). "Development and validation of an analytical model for perforated (multi-stage) regenerative M-cycle air cooler". In: *Applied Energy* 228, pp. 2176–2194. ISSN: 0306-2619. DOI: https://doi.org/10.1016/j.apenergy.2018.07.018. URL: https://www.sciencedirect.com/science/article/pii/S0306261918310456.

Underwood, C., M. Royapoor, and B. Sturm (2017). "Parametric modelling of domestic air-source heat pumps". In: *Energy and Buildings* 139, pp. 578–589. ISSN: 0378-7788. DOI: https://doi.org/10.1016/j.enbuild.2017.01.026. URL: https://www.sciencedirect.com/science/article/pii/S0378778817300774.

US Department of Energy (Sept. 23, 2021). *EnergyPlus Engineering Manual*. Version 9.6.0. Version 9.6.0 available online at https://energyplus.net/documentation.

Zanchini, E. and C. Naldi (2019). "Energy saving obtainable by applying a commercially available M-cycle evaporative cooling system to the air conditioning of an office building in North Italy". In: *Energy* 179, pp. 975–988. ISSN: 0360-5442. DOI: https://doi.org/10.1016/j.energy.2019.05.065. URL: https://www.sciencedirect.com/science/article/pii/S036054421930934X.

Zhao, X. et al. (2009). "Feasibility study of a novel dew point air conditioning system for China building application". In: *Building and Environment* 44.9, pp. 1990–1999. ISSN: 0360-1323. DOI: https://doi.org/10.1016/j.buildenv.2009.02.003. URL: https://www.sciencedirect.com/science/article/pii/S0360132309000419.

## ACKNOWLEDGEMENT

This publication is part of the R&D project PID2022-140796NA-I00 funded by MICIU/AEI/10.13039/501100011033 and by "ERDF A way of making Europe".



https://doi.org/10.52202/077185-0119